A98-31662 ICAS-98-5,11,1

ESTIMATION OF CIVIL AIRCRAFT PERFORMANCE AND OPERATING PRACTICES FROM RADAR DATA

R.E. Caves, L.R. Jenkinson *, D.P. Rhodes and J.B. Ollerhead †

Abstract

This paper responds to a need for an airport noise model to be driven by the recorded aircraft flight profiles and the resulting engine thrust settings. A method has been developed which transforms measured flight patterns to aircraft performance (e.g. speed and thrust) and operating procedures (e.g. flap settings or power changes). The method has been verified by comparison with flight data recording values obtained from aircraft at London Heathrow.

Throughout the study reference was made to the flight profile modelling procedures recommended by SAE (ref. 1), ECAC (ref. 2) and ICAO (ref. 3). As the SAE procedure is the predecessor of the other methods it has been used in the validation process. The standardised methods are employed in existing noise models in conjunction with aircraft manufacturers' databases. The most widely available is the FAA database which is supplied with the Integrated Noise Model (INM). The new procedure allows actual profiles from routinely gathered radar data to be used directly. Using this method reflects aircraft performance and operating practices more accurately than earlier methods which make several assumptions. The use of actual flight path allows consideration of non-reference flight conditions, for example the use of derated take-off thrust and variation in the height at which thrust is cut-back to climb-setting.

* Department of Aeronautical & Automotive Engineering & Transport Studies, Loughborough University, UK.
† Department of Operational Research and Analysis (DORA), National Air Traffic Services Ltd., London, UK.

Introduction

There are many different aircraft noise models currently in use around the world, many with 'local' factors incorporated but, basically, they all fall into one of two categories; empirical or deterministic. Empirical models rely on an empirical database acquired around the airports of interest, whilst the deterministic one synthesise representative flight profiles, usually building on data published or provided *ad hoc* by the manufacturers. The most widely used model is the US-FAA's Integrated Noise Model (INM) which falls in the second category and embraces modelling practices recommended by the SAE in AIR 1845 (ref. 1) and also incorporated in ECAC Document 29 (ref. 2) and ICAO Circular 205 (ref. 3). The most importance aspect of the INM is, perhaps, its unique database of aircraft performance and noise characteristics which has been assembled by the FAA over many years. The aircraft performance data is used in accordance with SAE 1845 to generate a set of 'standard' departure and arrival flight profiles for a selection of aircraft types at different takeoff masses. These profiles are not necessarily consistent with the profiles observed at particular airports and have to be adapted to reflect operational practices at the airport in question.

One reason why the operational flight profiles differ from 'standard' profiles lies in the fact that, these days, many airlines opt to conserve engine life by de-rating takeoff thrust in all but maximum weight, high temperature conditions, usually by preserving constant thrust/weight ratio. This is an important factor in determining take-off climb profile, but it cannot be related directly to standard INM conditions in which maximum takeoff thrust is normally assumed at the start of every operation.

There is therefore a need for an airport noise model to be driven by the observed aircraft flight profiles. This requires that realistic estimates of thrust levels are made from observed flight profiles which are readily available due to the widespread use of Noise and Flight Path Monitoring (NFPM) systems.

Development Process

Figure 1 shows the factors affecting aircraft flight profiles and thrust during a departure or arrival movement. The figure illustrates the flow of information

through the thrust estimation process and also a method for validation of thrust estimates computed from radar data. The flow of information begins with the definition of aircraft/engine type, sector details and ambient conditions. All these factors directly affect the departure height/speed profile. From the sector details, loading data is used to record takeoff mass. This may then be used to determine the takeoff thrust; in some instances the Flight Management System (FMS) will automatically set the required takeoff thrust based on aircraft mass and ambient conditions.

The profile flown is directly dependent on the engine performance characteristics, mass, operating instructions and aerodynamic characteristics of the aircraft. Operating instructions describe how the procedure is flown, both to monitor safety and also for noise abatement purposes. Instructions may define the initial flap setting, thrust cutback altitude, altitude for initial flap retraction and also the general inter-relationship between climb rate and acceleration. Additionally atmospheric factors such as windspeed and temperature also affect the flight profiles flown. Current modelling practice assumes that windspeed and direction remain constant with altitude.

Following the left side of figure 1, the aircraft departure profile is obtained from secondary surveillance radar (SSR). This provides aircraft position co-ordinates (x,y,z) as a function of time. From this, aircraft ground speed, longitudinal and normal acceleration, climb and bank angle may be derived. The data is then analysed using flight mechanics principles in conjunction with SAE-1845 to estimate aircraft thrust during the departure climb profile.

The right hand side of figure 1 illustrates how the Flight Data Recorder (FDR) is analysed to provide validation data. The FDR typically contains, true airspeed, ground speed, radar altitude, bank angle, flap setting etc. Engine thrust is not recorded directly, instead another engine parameter is recorded that may be converted to thrust using appropriate manufacturer data. For US manufacturers, fan speed (N1 percent) is commonly used to represent engine thrust. In contrast Rolls Royce engines use Engine Pressure Ratio (EPR). Aircraft position is recorded as latitude/longitude information. This is normally not accurate enough for comparison with radar position data and so FDR position information is computed by integrating speed and track angle information. The resulting data is used in conjunction with height and speed information to check accuracy of the radar data prior to thrust estimation. Finally the thrust outputs from the FDR and radar thrust estimation process are compared.

Theory

Figure 3 defines the forces acting on an aircraft during climbing and accelerating flight as observed for a typical departure movement. The forces shown are equally applicable to a landing aircraft where the aircraft is typically descending and decelerating.

For this analysis it is assumed that the thrust and drag forces are aligned parallel to the aircraft body axes. This approximation is suitable for aircraft at relatively low angles of attack. Resolving forces along the aircraft body axes it is possible to express aircraft thrust as:

$$T = D + Ma + Mg\sin\theta \qquad (1)$$

Thus it can be seen that aircraft thrust is the sum of three components, aircraft drag, acceleration and inertia/climb components. The latter two terms are simple to compute. The rate of acceleration and the climb angle can be obtained directly from radar data. Both terms however, are directly related to aircraft mass which is more difficult to estimate. It is often common to relate aircraft mass to the stage length flown, the greater the distance travelled, the greater the amount of fuel required. The relationship between takeoff mass and stage length is normally based on statistical databases of large numbers of flights. This however, masks day to day variations which may be ±20 percent of the mean value. Figure 2 shows the variation of takeoff mass with stage length for Boeing 747-400 operations departing London Heathrow. Additional operational effects of fuel tankering can significantly alter aircraft mass on certain routes relative to the statistical database.

The first term in equation (1), aircraft drag is rather more complex to estimate. Aircraft drag is dependent on ambient atmospheric conditions, airspeed and aircraft configuration. Ambient conditions can be estimated from altitude information.

Aircraft drag is expressed as a function of non-dimensional drag coefficient such that

$$D = \tfrac{1}{2}\rho V^2 S C_D \qquad (2)$$

The aircraft drag coefficient in equation (2) is implemented as a parabolic drag polar where

$$C_D = C_{D_0} + kC_L^{\,2} \qquad (3)$$

The first term in equation (3) represents the profile or shape drag coefficient of the aircraft. The last term

represents the drag due to lift and is a function of the induced drag coefficient, k, and the aircraft lift coefficient, C_L.

In level flight lift is assumed to be equal to the aircraft weight. However, during an accelerating climb lift is greater than the aircraft weight. The increase in lift is estimated using the normal load factor defined as,

$$n = 1 + \frac{a_N}{g} \qquad (4)$$

where a_N is the vertical acceleration computed from radar data and g is the acceleration due to gravity.

During a departure or arrival operation the aircraft configuration changes; during departures flap angle is reduced as the flaps are retracted. During arrival operations, flap angle increases to reduce approach speed and undercarriage is also extended. These effects change the aircraft drag characteristics and hence aircraft thrust computed using equation (1). Flap and undercarriage changes alter the aircraft profile drag coefficient in equation (3). Defining the point of aircraft configuration changes is a complex task. Pilot manuals contain flap/speed schedules which are designed to provide adequate stall speed margin in all configurations. In this study FDR analysis was undertaken to determine if flap/speed schedules could be used to estimate flap angle as a function of speed for actual operations. Table 1 shows results from the analysis of fifty Boeing 757 arrivals.

Flap Angle (°)	Avg. Speed (knots)	Standard Deviation (knots)
5	193	10
15	180	12
20	170	9
25	151	7
30	139	20

Table 1: Flap/Speed Schedule

For certain aircraft, the Boeing 747-400 in particular flap changes have been identified to precede rapid changes of speed. This enables the change to be pin-pointed using radar derived speed profiles. However, the actual flap setting must be still be deduced using appropriate flap/speed schedule data.

Turning Flight

The forces acting on a aircraft in steady turning flight are shown in figure 4. During turning flight, the lift vector is not vertical and additional lift must be produced to compensate for this increasing aircraft drag.

Resolving forces in the plane of the wing gives,

$$Mg\sin\phi = \frac{Mv^2}{R}\cos\phi \qquad (5)$$

Resolving normal to the wing plane gives,

$$L = Mg\cos\phi + \frac{Mv^2}{R}\sin\phi \qquad (6)$$

Equation (5) reduces to,

$$\tan\phi = \frac{v^2}{Rg} \qquad (7)$$

Noting that $L = n_t Mg$, equation (6) reduces to,

$$n_t = \cos\phi + \tan\phi\sin\phi \qquad (8)$$

The load factor computed using equation (8) is then multiplied by the normal load factor to produce the overall aircraft load factor for climbing/descending and turning flight. In order to use equation (8), aircraft bank angle, ϕ must first be computed using equation (7). This requires aircraft speed which is readily obtained from radar data. The track radius is obtained from radar data by solving the coefficients of the general function of a circle,

$$x^2 + y^2 + 2gx + 2fy + c = 0 \qquad (9)$$

where the origin is (-g,-f) and the radius is,

$$r = \sqrt{f^2 + g^2 - c} \qquad (10)$$

In order solve equations (9), and (10), three pairs of (x,y) co-ordinates are required to determine the coefficient, c, f and g. Thus the turn radius at x(t), y(t) is computed using the additional co-ordinates x(t-Δt), y(t-Δt) and x(t+Δt), y(t+Δt).

It is important to note that the load factor due to turning flight is not dependent on aircraft mass. The effect is also highly non-linear as shown by the values in table 2 computed from equation (8).

ϕ	n_t
0	1.000
10	1.015
20	1.064
30	1.155

Table 2: Load factor during turning flight

Below Radar Estimation

Many radar systems are unable to output complete data describing the aircraft position as a function of time from the start of the takeoff roll. Reflections and distortions often occur from obstacles at heavily developed airfields disrupting radar coverage. In such circumstances it is common for the radar system to filter out data below certain heights. This leaves a portion of the flight profile, typically when the aircraft is at its highest power setting where aircraft position and thrust are unknown.

Provided radar data is available at a point during the initial climb phase it is possible to extrapolate backwards. During this phase it may be assumed that aircraft climb gradient and speed are approximately constant. Ignoring the circular arc flight path near rotation this enables the point of lift-off to be estimated. If the start of roll point is known the ground distance can be determined directly. However, in some instances intersection takeoffs may be used where the start of roll point is not known. It is then possible to estimate the start of roll by computing the ground roll distance using the SAE-1845 method and using the thrust computed from the initial radar points during the initial climb phase.

Results

Figures 5 and 6 show the results taken for two Boeing 737-400 departures. Figures 6 and 7 show the results for two Boeing 747-400 departures. Figures 9 and 10 show the results for two Boeing 747-400 arrivals.

The results illustrate clearly that aircraft thrust settings can be estimated from radar data for both the Boeing 737-400 and the Boeing 747-400. In addition to these aircraft, Boeing 767-300 aircraft have also been analysed with similar results. Figure 5-8 also show the magnitude of the three components contributing to total aircraft thrust. For both aircraft it can be seen that the contribution of drag, acceleration and climb angle are approximately equal. This was not expected, but is perhaps a logical result. During a departure the pilot is concerned with increasing airspeed and altitude. With a finite amount of excess thrust for acceleration and climb, it is logical that in these cases the pilot has chosen to split the excess thrust equally between the needs of acceleration and climb.

Figures 9 and 10 show that the thrust may be estimated with equal accuracy for arrivals operations. In this mode of flight, however, aircraft drag is far more significant compared with the contributions due to decelerating and descending flight. This places greater emphasis on aircraft configuration and drag coefficient data which all affect the total aircraft drag. For arrivals operations below radar estimation is considerably simpler as the aircraft glideslope and speed are generally held constant during final approach.

Finally, figure 11 shows the estimated aircraft bank angle compared with FDR output. Correlation is very good the maximum difference being approx. 4° during short turns. This is partly a symptom of the smoothing process, which tends to reduce the peak bank angle particularly during short turn manoeuvres.

Input Data Issues

Critical to the thrust estimation process is the quality of the radar data used. For this study the radar data has a basic x,y resolution of 1/16nm (115m). Prior to receiving the radar data it was smoothed. The resulting data was still not sufficiently smooth for the computation of second derivatives (acceleration). Thus additional smoothing was performed using techniques presented by Roberts et al (ref. 4). Additional work is still needed in this area as some degree of oscillation remains in the computed acceleration values.

The radar update rate for the data used was 3.8 seconds. Since both the first derivative of the position data (speed) and the second derivative (acceleration) are required it is desirable to use faster update rates. With advancements in radar technology including back-to-back radar antennae update rates of only 1 second are now possible.

Conclusions

The paper describes the importance of accurate thrust profiles for noise modelling research and also the possible variability in operational thrust profiles. To account for this variability a method is presented that enables the thrust profile from an individual flight to be

estimated. The method computes the thrust due to drag, acceleration and climb effects. In addition the effects of turning flight are also incorporated. Encouraging results are shown for Boeing 737-400, Boeing 747-400 departure operations and Boeing 747-400 arrival operations. The method has also been successfully applied to Boeing 757-200 arrival operations.

With the increasing availability of radar data with improved quality levels it is envisaged that the overall accuracy of the method can be improved and enable the routine processing of individual flight tracks for use in historical noise contour modelling.

References

1. Society of Automotive Engineers (SAE), "Procedure for the Calculation of Airplane Noise in the Vicinity of Airports", Aerospace Information Report AIR 1845, January 1986.
2. ECAC, "Standard Method for Computing Noise Contours around Civil Airports", ECAC Document 29, Amendment 1 September 1987.
3. ICAO, "Recommended Method for Computing Noise Contours around Airports", ICAO Circular 205-AN/125.
4. Roberts, S., McLeod, R., Vermij, M., Heaslip, T. and MacWilliam, G., "RAP (Radar Analysis Program) - An Interactive Computer Program for Radar Based Flight Path Reconstruction and Analysis, p.27-45, Seminar Proceedings, ISASI forum 1994.

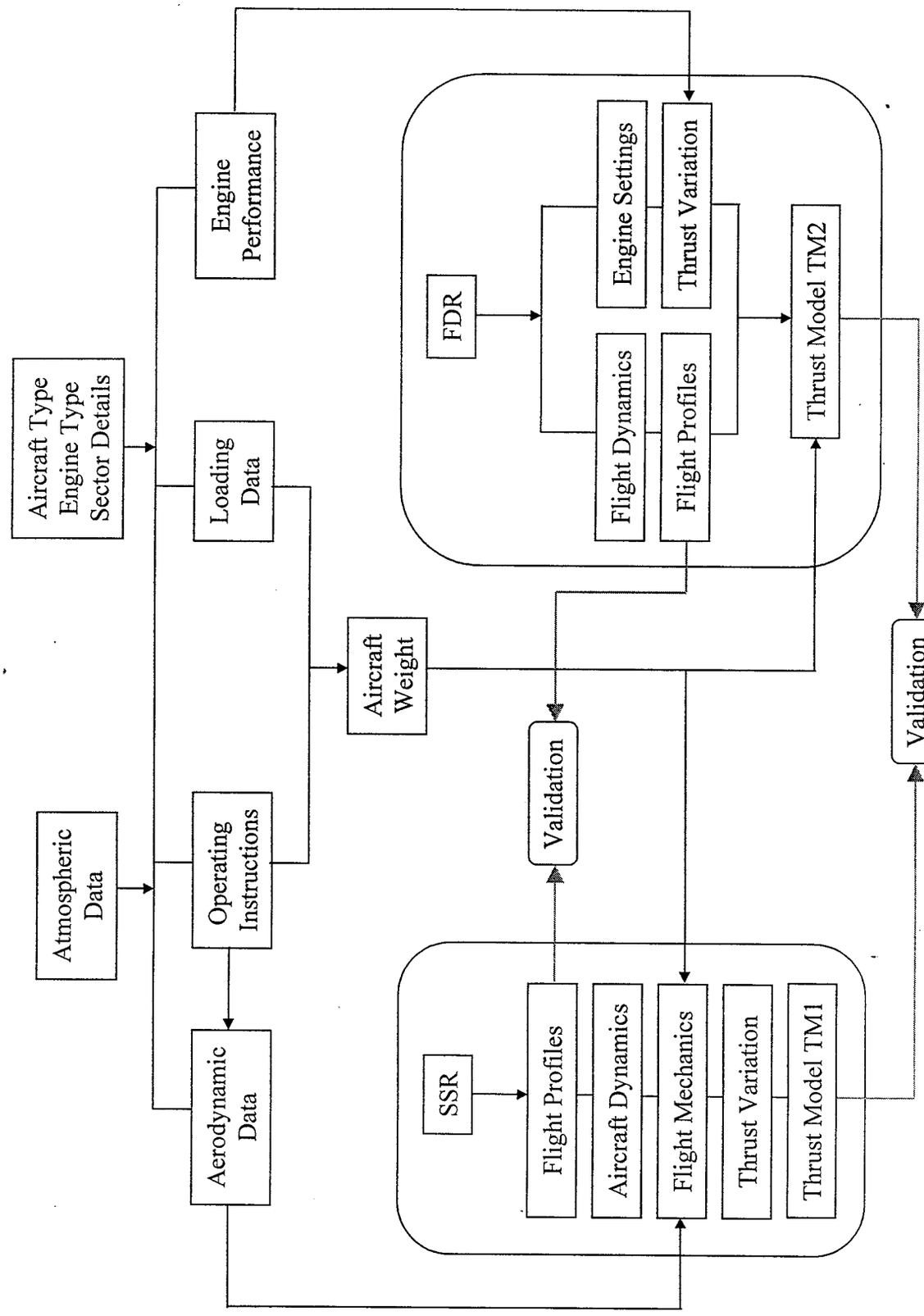

FIGURE 1: Thrust Modeling Information Flow

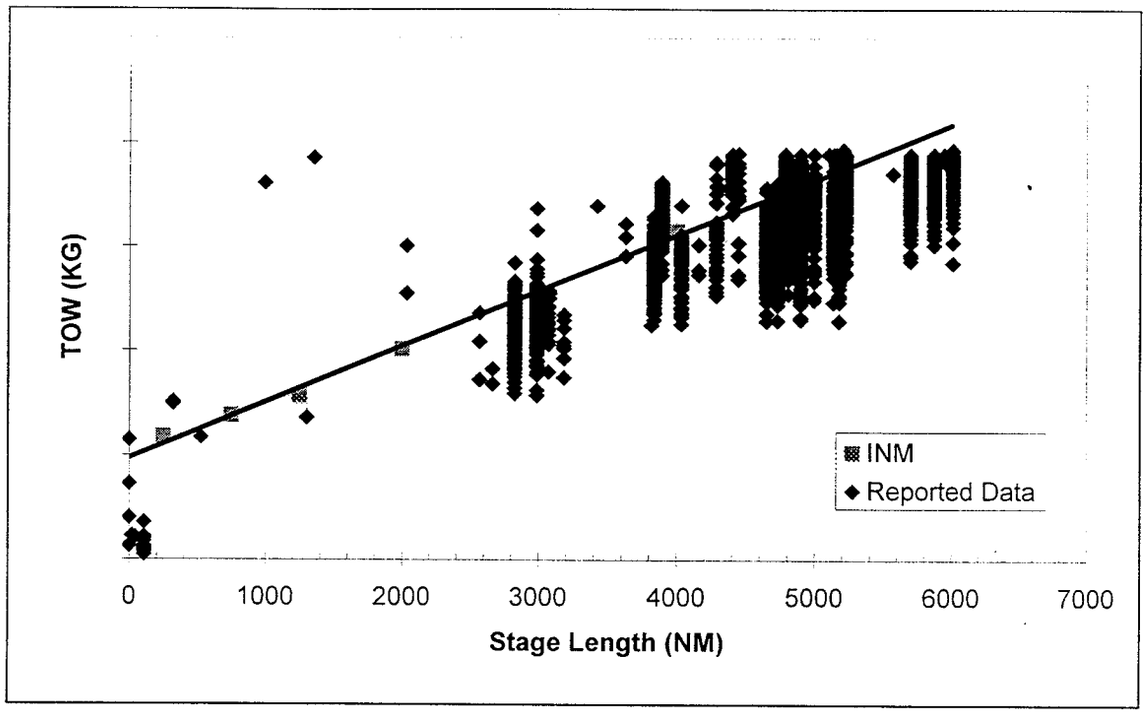

FIGURE 2: Correlation of Stage Length and Takeoff Weight

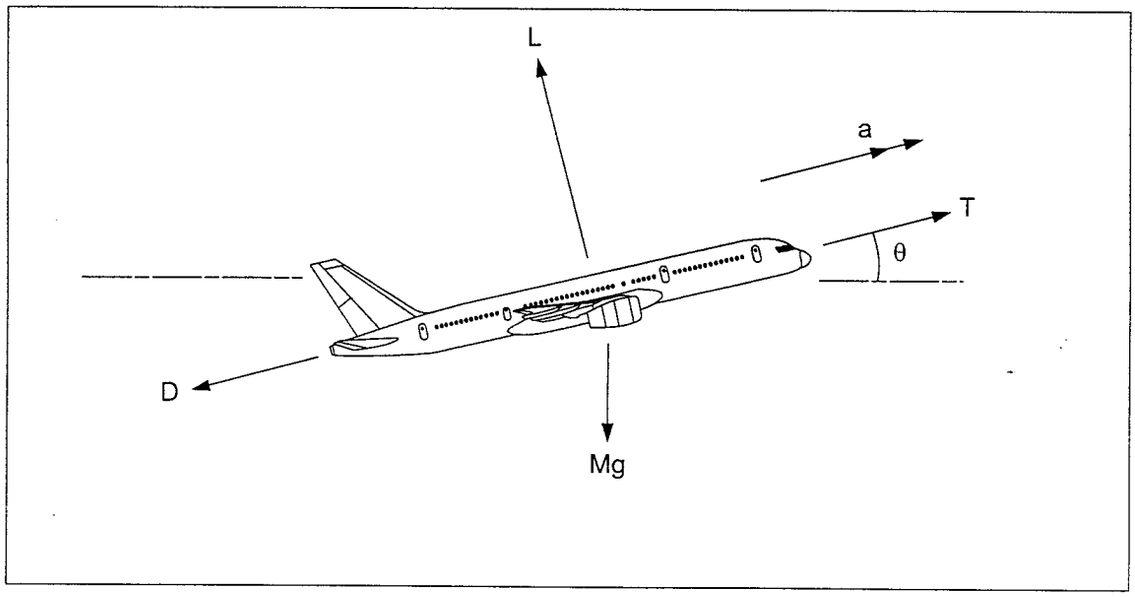

FIGURE 3: Forces acting on a climbing accelerating aircraft

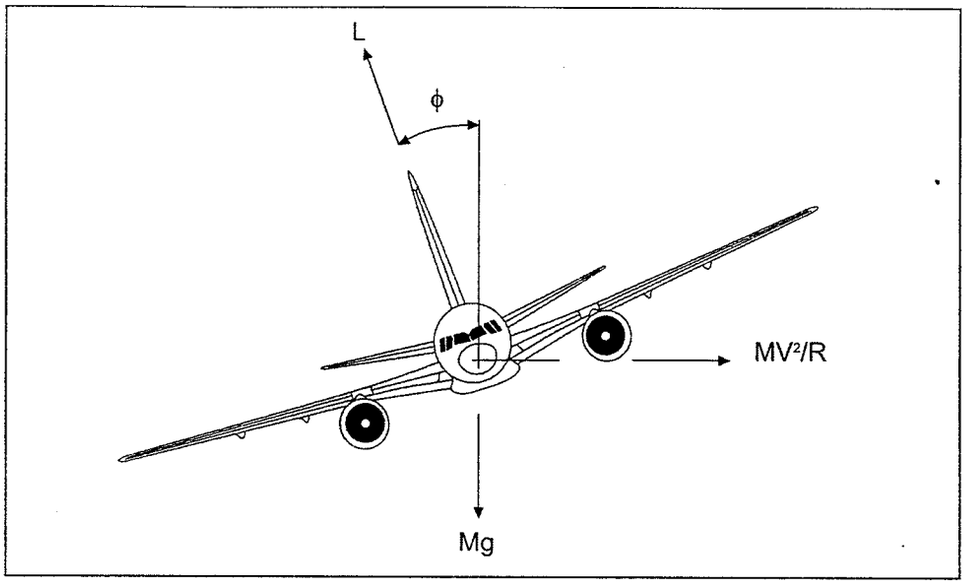

FIGURE 4: Forces acting on turning aircraft

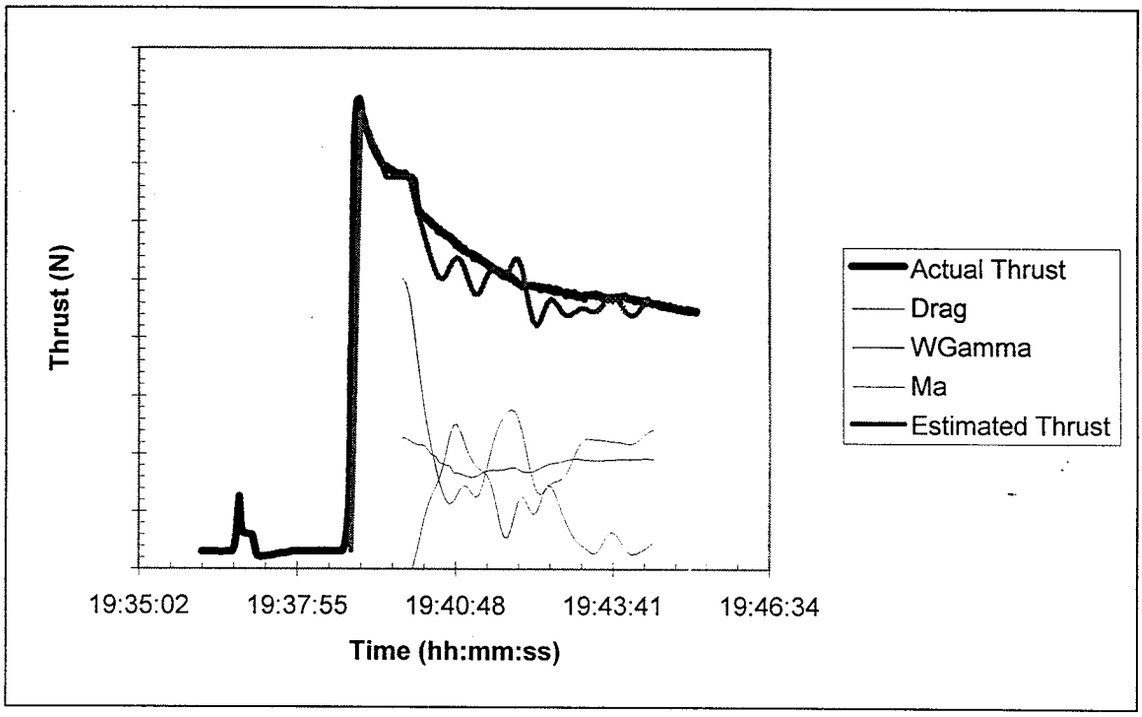

FIGURE 5: Boeing 737-400 Departure

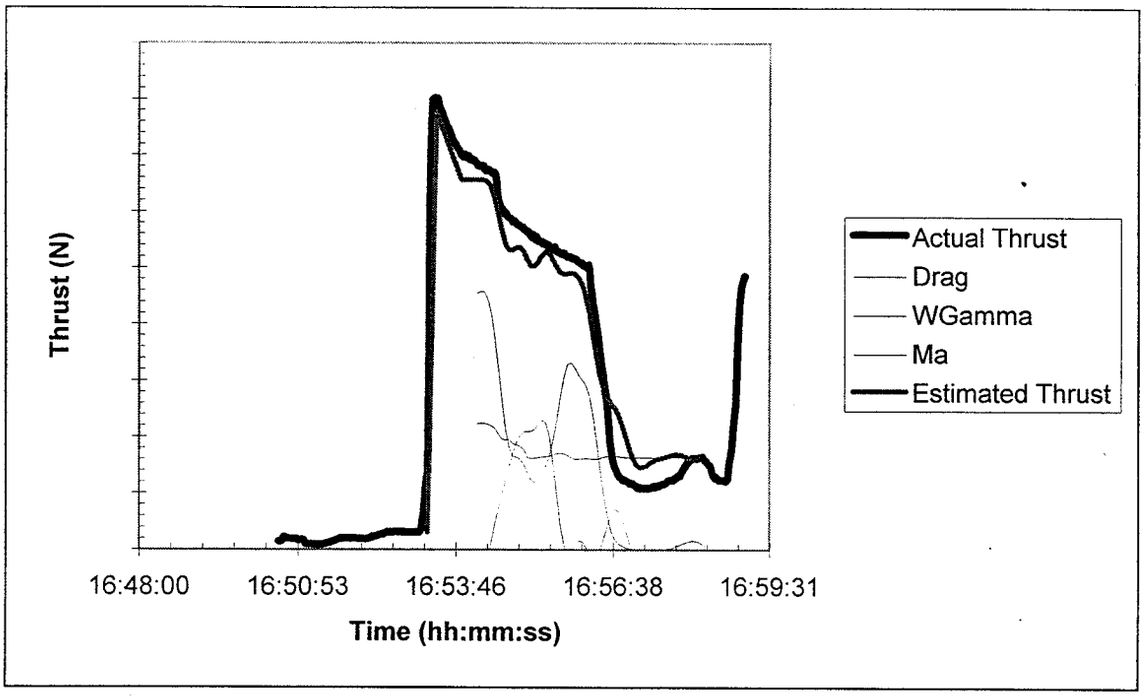

FIGURE 6: Boeing 737-400 Departure

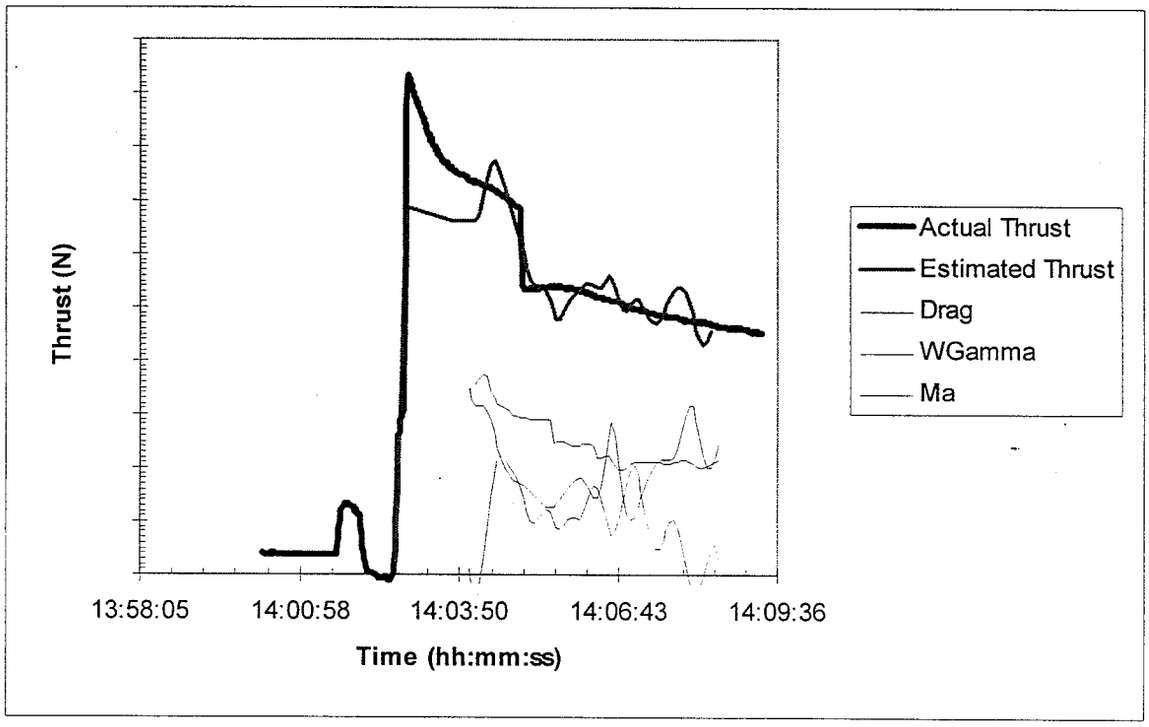

FIGURE 7: Boeing 747-400 Departure

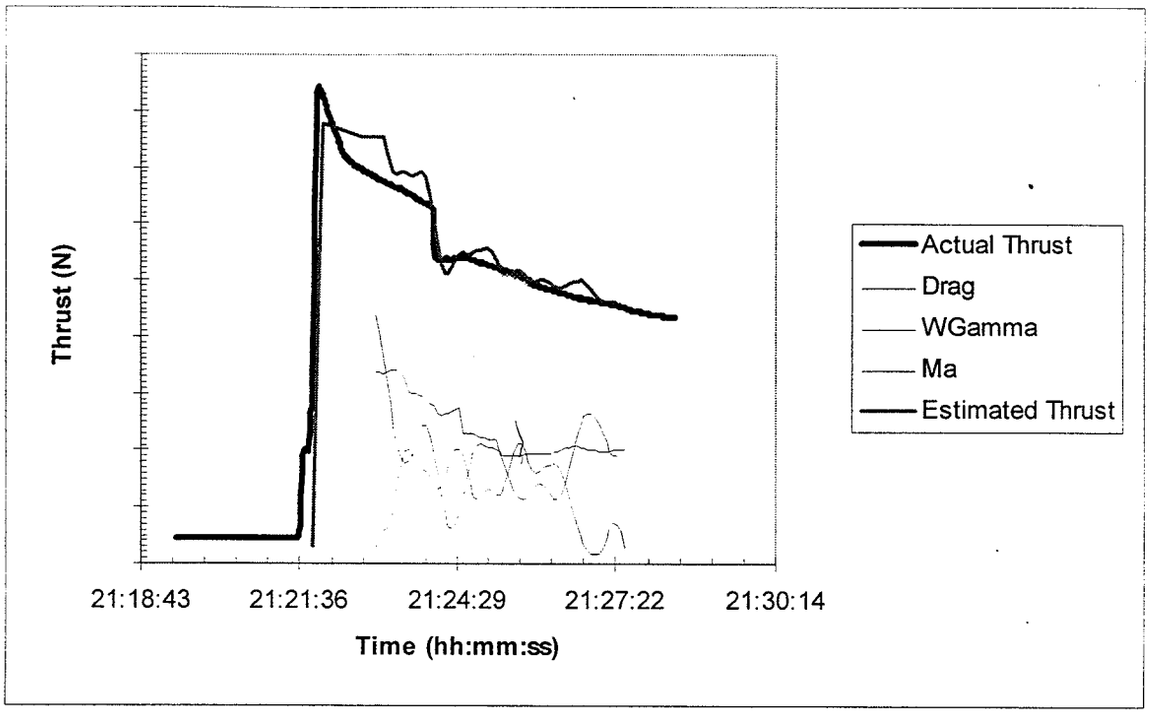

FIGURE 8: Boeing 747-400 Departure

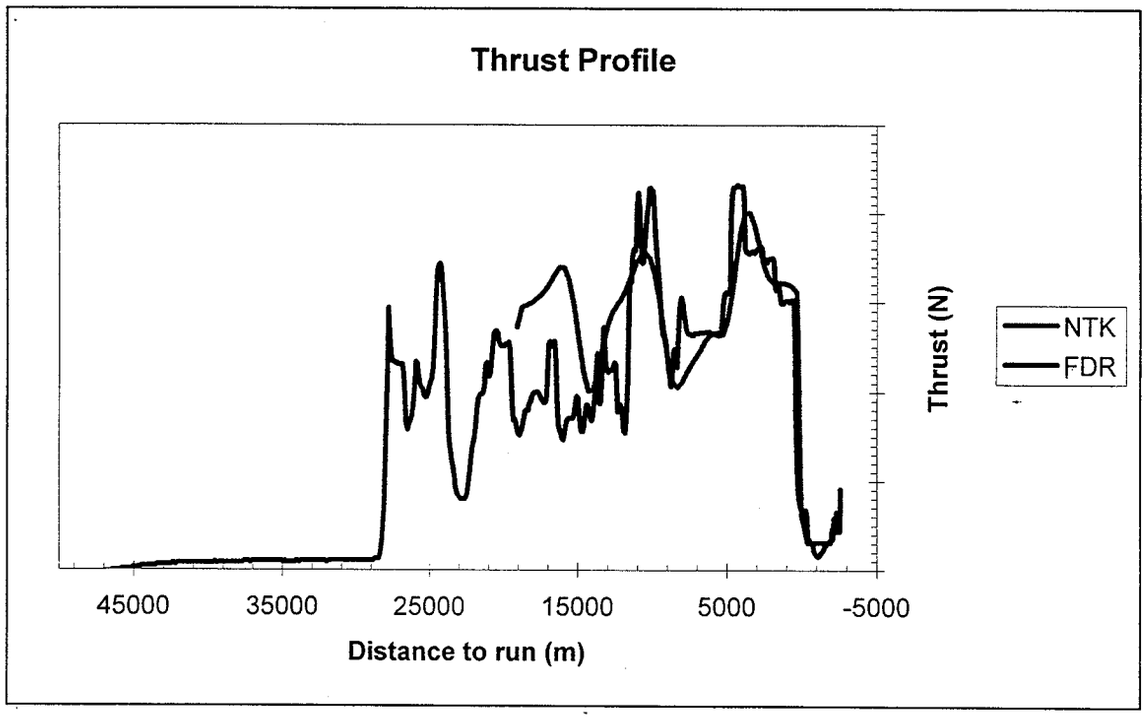

FIGURE 9: Boeing 747-400 Arrival

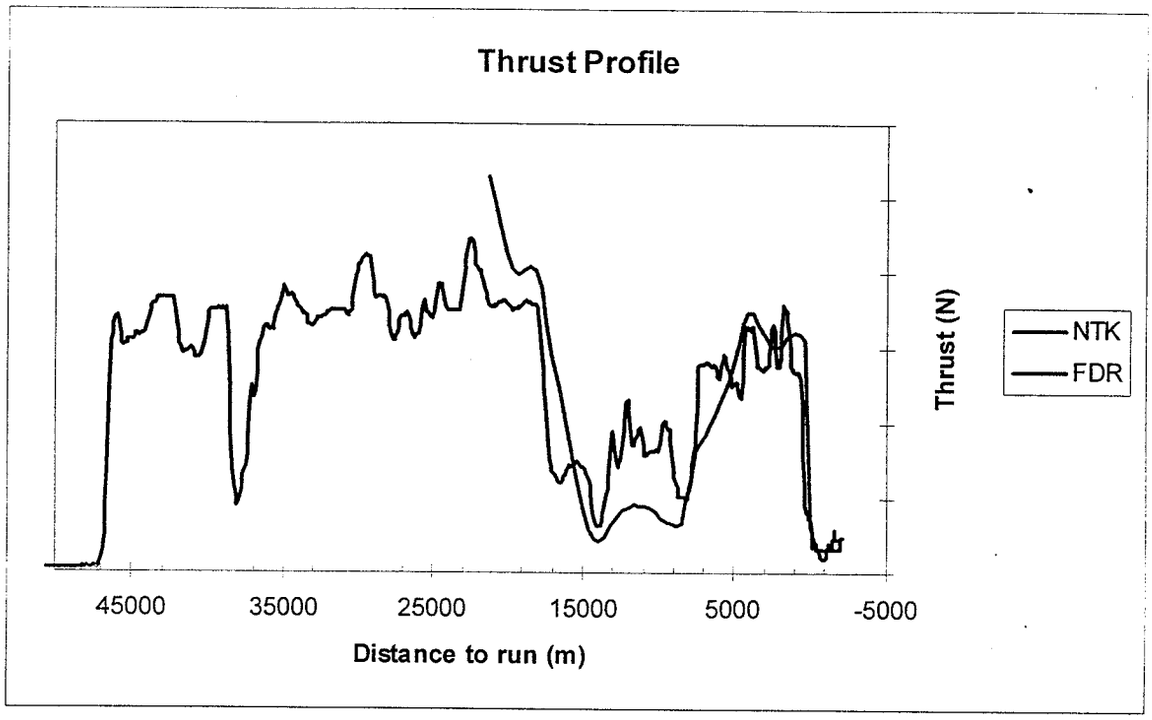

FIGURE 10: Boeing 747-400 Arrival

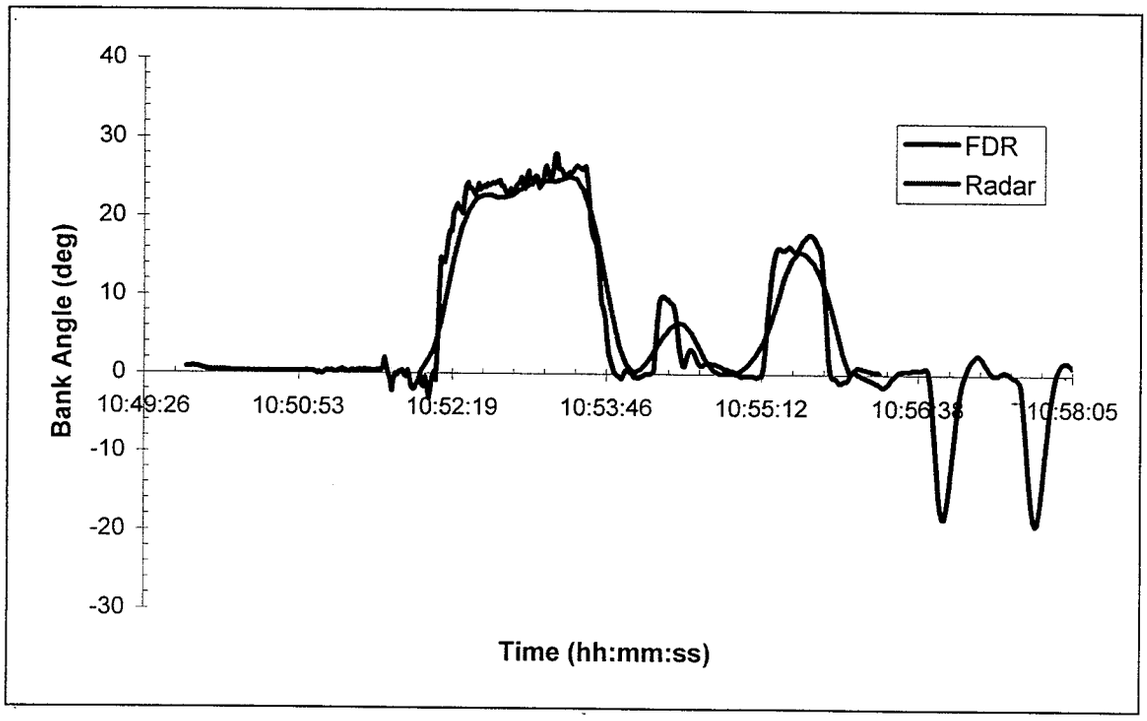

FIGURE 11: Boeing 767-300 Bank Angle Correlation